View Article Online
View Journal

Green Chemistry

Cutting-edge research for a greener sustainable future

Accepted Manuscript

This article can be cited before page numbers have been issued, to do this please use: T. Thiebault, J. Brendle, G. Auge and L. Limousy, *Green Chem.*, 2019, DOI: 10.1039/C9GC02243K.

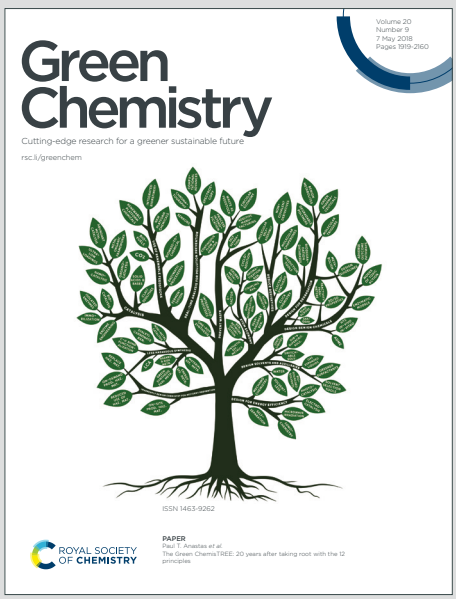

ROYAL SOCIETY OF CHEMISTRY

rsc.li/greenchem

View Article Online
DOI: 10.1039/C9GC02243K

ARTICLE

Zwitterionic-surfactant modified Laponites® for removal of ions (Cs^+; Sr^{2+} and Co^{2+}) from aqueous solution as a sustainable recovery of radionuclides from aqueous wastes

Received 00th January 20xx,
Accepted 00th January 20xx

DOI: 10.1039/x0xx00000x

Thomas Thiebault,*[a,b,c] Jocelyne Brendlé,[a,b] Grégoire Augé[d] and Lionel Limousy[a,b]

The synthesis of zwitterionic-surfactant modified Laponites® (LAP-CBs) was investigated as a function of the surfactant loading in order to obtain suitable adsorbent for the removal of Co^{2+}, Sr^{2+} and Cs^+ ions from aqueous solutions. The proper adsorption of surfactant was characterized by several techniques allowing to emphasize the modification of the surfactant distribution between the interlayer space and the surface of Laponite® (LAP), with increasing the load of surfactant. The organophilic character of the obtained LAP-CBs strongly affected its affinity with the targeted contaminants. The adsorption of Sr^{2+} was lowered onto LAP-CBs in comparison to LAP, while the adsorption of Co^{2+} and Cs^+ were strongly improved. The competition between Sr^{2+} and Cs^+ was important onto LAP-CBs, whereas no competition was found when using LAP, indicating different adsorption mechanisms depending on the adsorbent. The desorption of contaminants was performed in various solutions and confirmed these mechanisms. Whereas Cs^+ and Sr^{2+} were adsorbed through cation exchange onto LAP-CBs, as highlighted by a significant desorption in saline solution, the desorption of Co^{2+} from LAP-CBs was very poor whatever the composition of the solution indicating rather a complexation. Finally, the increase of the load of surfactant decreased the adsorption capacity of all the investigated contaminants. The arrangement of the surfactant, within the interlayer space or on the surface of LAP, was therefore of high concern when considering the potential of this material to durably remove radionuclides from low-level radioactive wastewaters.

Introduction

The production of electricity by nuclear power plants generates significant amounts of radioactive wastes.[1] These wastes are currently managed by containment from their environment in various conditions depending on the level and the half-life of the radionuclides.[2] The production of low-level radioactive wastes (LLRW) is the most important in volume due to the constant discharge of contaminated effluents by nuclear power plants.[3]

The management of LLRW represents an important challenge due to the hardness for treating such complex effluents with economically viable productions. However, reaching a suitable solution for the decontamination of LLRW is of high concern in order to avoid the environmental dispersion of hazardous radionuclides.[4] With this aim, adsorption could represent a potential way to adsorb radioactive inorganic cations if the selected adsorbent presents both appropriate adsorption properties and reasonable costs.[5,6] Several materials and processes have been tested in order to adsorb radionuclides, such as zeolites,[7,8] oxides,[9] membranes,[10] or clay-based adsorbents.[11–13]

Clay minerals are among the most abundant and cheapest materials, and they are especially recognized for the adsorption of cationic contaminants given their cation exchange capacity (CEC).[5,14,15] This structural property, associated with a very low hydraulic conductivity,[16,17] results in the promotion of this material for the long-term geological storage of high-level radioactive wastes.[18,19] Nevertheless, the use of natural clays could represent a risk considering the possible chemical variations and the presence of undesired substitutions in the extracted clay minerals.[20,21] Synthetic clay minerals could therefore represent an added-value, resulting from their stable chemical composition.

One of the main limitation of clay minerals is their poor selectivity depending on the targeted contaminant. Liquid effluents originating from nuclear power plants are complex solutions, as they contain various inorganic cations (*e.g.* radionuclides) as well as organic matter or surfactants that could hinder the adsorption properties of clay minerals.[22] Therefore, raw clay minerals could be inappropriate for an efficient fixation of such contaminants.

In order to improve the selectivity and/or the affinity of clay-based adsorbents in relation to specific ions, several papers have demonstrated that their organo-modification could be

[a] Université de Haute-Alsace, IS2M, CNRS, UMR 7361, 3b rue Alfred Werner, F68100, Mulhouse, France.
[b] Université de Strasbourg, France
[c] EPHE, PSL University, UMR 7619 METIS (SU, CNRS, EPHE), 4 Place Jussieu, F-75005, Paris, France
[d] ONET Technologies, 36 Boulevard de l'Océan, CS 20280, 13258, Marseille Cedex 09, France
*mail: thomas.thiebault@ephe.psl.eu
† Footnotes relating to the title and/or authors should appear here.
Electronic Supplementary Information (ESI) available: [details of any supplementary information available should be included here]. See DOI: 10.1039/x0xx00000x

beneficial.[23–27] The organo-modification of clay minerals can be carried out with various type of organic compounds such as surfactants. Each type of surfactant (*i.e.* cationic, anionic, non-ionic and zwitterionic) allows the organophilisation of the interlayer space of the clay minerals. However, only cationic and zwitterionic surfactants lead to a strong affinity with the clay mineral. Their intercalation within the layers of the clay minerals is performed through cation exchange ensuring a stable and energetic adsorption of the surfactant. Yet, only zwitterionic surfactants could maintain the cation exchange capacity of the resulting organo-modified clay minerals, due to its zwitterionic charge.[28,29] Conversely, the intercalation of cationic surfactants could hinder the cation exchange capacity by compensating the negative surface charge of clay minerals.[30,31]

The innovative approach of this research stands in the use of Cocamidopropyl Betaine (CB), a widely-spreaded low cost zwitterionic surfactant used as intercalated agent. CB is currently employed in various cosmetic products due to its safety and biodegradability,[32] and it has also been proposed for the treatment of wastewaters, due to its chemical properties.[33] A commercially available synthetic hectorite (Laponite® RD, LAP) was selected as host materials to prepare a series of hybrids having different surfactant load, the goal of this study being to prepare adsorbent by an environmental friendly way, i.e. by using water as solvent and heating at low temperature (40°C at maximum). The adsorption of ^{133}Cs, ^{59}Co, ^{88}Sr, three stable radionuclides isotopes commonly detected (*i.e.* of ^{137}Cs, ^{60}Co and ^{90}Sr, respectively) in LLRW was then investigated on LAP and on the CB modified LAP (LAP-CBs). The influence of the surfactant loading on the adsorption properties of Co^{2+}, Sr^{2+} and Cs^{+} of LAP-CBs was deciphered as well as the competitive adsorption and desorption of the contaminants in various type of solutions. These latter experiments underlined that the developed adsorbents may be suitable to replace the complex matrixes used for the removal of radionuclides from aqueous solution.

Materials and Methods

Chemical reagents

Raw Laponite® RD (LAP) was purchased to BYK company and was used without further modification. Zwitterionic surfactant, Cocamidopropyl Betaine (CB) was supplied by APC Pure Chemical Company assuming a minimal surfactant content of 30%. General information as well as the distribution of CB species as function of pH are presented in Table S1 and Figure S1 respectively.

Cesium chloride (CsCl, >99.99%), Strontium hexahydrated Chloride ($SrCl_2.6H_2O$, >99%) and Cobalt hexahydrated chloride ($CoCl_2.6H_2O$, >98%) were supplied by Carl Roth company.

Chemical reagents such as HCl, NaOH, NaCl and $CaCl_2$ were supplied by Sigma-Aldrich company at analytical grade and were used without further modifications.

Synthesis of zwitterionic-surfactant modified Laponite®

The protocol for the modification of raw LAP was the following. 5 g of LAP were mixed with various amounts of surfactant relating to the cation exchange capacity (CEC) of LAP (*i.e.* 75 meq $100g^{-1}$) in a 200 mL solution of acidified pure water (adjusted with 0.1 M HCl to obtain pH = 3). Four different CB amounts were used corresponding to 0.5, 1, 2 and 4 CEC of LAP respectively. After the addition of CB, the solution was continuously stirred with magnetic stirrer at 200 rpm during 24 hours and at 40°C.

The solid material was then recovered by centrifugation at 8,000 rpm during 10 minutes. The material was rinsed two times with pure water and recovered by centrifugation at 8,000 rpm during 10 minutes. Then, the material was dried in an oven at 60°C during 72 hours.

Hereafter, each adsorbent is labelled according to the CB load during synthesis (i.e. which is not the adsorbed amount of CB onto LAP).

Experimental techniques

X-ray diffraction (XRD) patterns of the different samples were recorded on a PANanalytical X'Pert Pro MPD diffractometer using Cu Kα radiation (λ = 1.5418 Å) and Θ-2Θ mounting (Bragg-Brentano geometry). Measurements were achieved for 2Θ angles values between 2 and 70°, step 0.17° 2Θ.

Fourier transform infrared (FTIR) measurements in the range 400-4000 cm^{-1}, were recorded using a Bruker 55 FT-IR spectrometer equipped with Nd: YAG laser operating at 1064 nm and a Ge detector. The analyses were performed in transmission mode and each spectrum was the average of 256 scans collected at 2 cm^{-1} resolution.

Thermogravimetric (TG) analyses were performed on a TG Mettler Toledo STARe apparatus under air flow with a heating rate of 2°C min^{-1} from 30 to 900°C. All samples were air-dried during 48 hours in order to obtain comparable hydration state.

Zeta potential (ZP) measurements were realized using a Malvern Nanosizer instrument. 20 mg of material were dispersed in 50 mL of a 10^{-3} M NaCl solutions. The pH of the suspension was adjusted using 0.1 M NaOH and/or HCl solutions and the suspension was stirred for 24 h until ionic equilibrium was reached.

The concentrations of the different cations (Cs^{+}, Co^{2+} and Sr^{2+}) were quantified with atomic absorption spectroscopy (Varian AA 240 FS), using the absorption mode and acetylene as fuel.

Adsorption experiments

Adsorption experiments were carried out both in single-solute and in competitive solutions. Typically, the adsorbent mass was 100 mg in 100 mL of solution spiked with different amounts of contaminant solution. The concentration of each contaminant ranged from 6 to 600 µM for Cs^{+}, 4.2 to 420 µM for Co^{2+} and 3.7 to 370 µM for Sr^{2+} in both single-solute and competitive solutions, in pure-water solution spiked at 100 µM of NaCl. The pH value of each isotherm solution was let free and measured at the beginning and at the end of interaction (*i.e.* 6-6.5). Solutions were then centrifuged at 8,000 rpm during 5 minutes and the contaminant concentration in supernatant was analyzed by atomic absorption spectroscopy.

The impact of pH on the adsorption capacity of single-solute solutions of Cs^+, Co^{2+} and Sr^{2+} was carried out with the same protocol. The only difference was that the pH of the solution was modified with 1M HCl and/or 1M NaOH solutions in order to obtain a range of pH values between 2 and 12.

Desorption experiments

After interaction with contaminants, the adsorbents were recovered by centrifugation at 8,000 rpm during 10 minutes. The recovered material was then dried at 60°C during 72 hours. 20 mg of dried adsorbent were then mixed with 20 mL of three different solutions; Pure water, 1 mM of $CaCl_2$ and 2 mM of NaCl. The solution was then gently stirred during one week at room temperature. Solutions were then centrifuged at 8,000 rpm during 5 minutes and the contaminant concentrations in supernatant were analyzed by atomic absorption spectroscopy.

Sorption modeling

The fitting of the resulting adsorption isotherms by using Langmuir, Freundlich and Dubinin-Radushkevich (DR) equation models drives to thermodynamic parameters allowing one to precisely quantify the affinity of contaminants with the sorbent. Briefly, Langmuir model is expressed by the following equation:[11,14]

$$q_{ads} = \frac{q_{max} K_L C_{eq}}{1 + K_L C_{eq}}$$

Where q_{ads} is the equilibrium amount adsorbed on sorbent (mmol.g^{-1}), C_{eq} the equilibrium concentration in the supernatant (mmol.L^{-1}), q_{max} the adsorption capacity of the sorbents (mol.g^{-1}) and K_L is the Langmuir adsorption constant (L.mol^{-1}) which is related to the free energy ($\Delta G°$) of adsorption. The linear Freundlich model equation is written as follow:[14,34]

$$lnq_{ads} = lnK_F + \frac{1}{n} lnC_{eq}$$

where K_F (mg.g^{-1})/(mg.L^{-1})^n and n are the Freundlich constants indicating the extent of the adsorption and the degree of nonlinearity between contaminants and the adsorbent respectively. The linear expression of the DR model used to adjust our experimental data is expressed as follow:[23,35]

$$lnq_{ads} = lnq_m + \beta\varepsilon^2$$

where ε corresponds to the Polanyi potential of which relation including C_{eq} the equilibrium concentration could be found elsewhere. The constant β corresponds to the activity coefficient associated to the mean free energy E (kJ.mol^{-1}) described by the following equation:[23,35]

$$E = (2\beta)^{-1/2}$$

This later parameter gives information whether the adsorption mechanism involves a cation exchange or physical adsorption. Indeed, if the magnitude of E is below 8 kJ mol^{-1}, physisorption is envisaged, while for E > 8 kJ mol^{-1} the adsorption process follows chemisorption.[11,14]

Results and Discussion

View Article Online
DOI: 10.1039/C9GC02243K

Characterization of LAP and zwitterionic-surfactant modified Laponite®

The LAP and zwitterionic-surfactant modified LAPs (LAP-CBs) were characterized by XRD, FTIR and TG/DTG analyses. The *00l* diffraction patterns of LAP-CBs shift to lower angular values in comparison with LAP, underlining the intercalation of surfactant within the interlayer space of the starting clay mineral.

LAP exhibits a *00l* reflection at 7.0° (2θ) leading to an interlayer spacing of 13.7 Å (Figure 1).

As expected, with a CB load of 4 times the CEC of LAP, the interlayer space increases, reaching 22.3 Å. This value matches with an organization of the surfactant in paraffin monolayer structure.[36,37] Considering the basal spacings of LAP-CBs, the arrangement of the surfactant is expected to be a monolayer at 0.5 and 1 CEC, and a pseudo-trilayer at 2 CEC.[36] FTIR spectra of LAP-CBs show typical features characteristics of the organic compounds: the absorption bands at 2840-2920 cm^{-1} are relative to the symmetric and antisymmetric CH_2 stretching vibrations of the CB aliphatic chain (Figure S2). The presence of these bands testifies the proper adsorption of CB onto LAP.

Three main domains of weight losses can be expected from TG analyses of LAP-CBs. Below 150°C, the loss of weight is due to the evaporation of free and adsorbed water; between 150 and 600°C occurs the devolatilization and the thermal oxidation of organic matter (OM), and beyond this temperature, dehydroxylation of LAP is expected.[38] TG analyses of LAP and LAP-CBs exhibit two distinct patterns (Figure S3). With the increase of the CB load, a decrease of the weight loss associated to water content (*i.e.* T = 38-46 °C) is observed.

Conversely, the loss of weight associated with the organic content strongly increases with the CB load (*i.e.* T= 230-319°C). The DTG curves illustrate these qualitative information too, but also indicates the doubling of the peak associated with the thermal decomposition of organic matter (*i.e.* CB, Figure 2). This doubling can be explained by the distinction between CB adsorbed onto the surface of the clay mineral (*i.e.* lower temperature) and intercalated CB (*i.e.* higher temperature).[28,39] Quantitative data can be derived from these curves and are expressed in Table S2.

As observed in Figure 2 and Table S2 the water content decreases with increasing CB amount from 13.7% for LAP to 4.0% for LAP-CB-4CEC respectively. The weight loss associated to CB thermal oxidation can be calculated for a global weight loss considering the total amount of adsorbed CB (*i.e.* 150-550°C), or split between surfactant adsorbed onto the surface or intercalated (Figure 2). The total OM content ranges from 4.9 % at 0.5CEC of surfactant load and 29.1% at 4CEC of surfactant load. These values allow calculating the adsorbed amount of CB that represents 0.21, 0.39, 0.84 and 1.10 times the CEC of the LAP at 0.5, 1, 2 and 4CEC of surfactant load respectively (Figure 3). The amount of adsorbed CB is therefore higher for higher initial loads of CB. It should be noted that the amount of adsorbed CB slightly exceeds the CEC of LAP for LAP-CB-4CEC, exhibiting the potential recombination between the surfactant

molecules. This increase of CB content is not equally distributed on LAP-CBs. As showed in Figure 3, there is a sudden increase of the surface adsorption between 1 and 2 CEC of CB loads.

The amount of CB adsorbed onto the surface is even equal to the intercalated amount at 4 CEC. The intercalated amount of CB exhibits a weak increase between 2 and 4 CEC, with such a saturation around 0.5 CEC of LAP (Table S2). As a result, the CEC is not the only limiting factor for the intercalation of CB within the layers. The possible impact of a steric hindrance could be highlighted. This result was previously observed with other zwitterionic surfactants intercalated within montmorillonites, for which the maximal intercalated amount reached 0.6 CEC.[39]

Zeta potential (ZP) values of LAP, LAP-CB-0.5CEC and LAP-CB-4CEC were evaluated as a function of the pH. ZP values of LAP are very close to 0 in a wide range of pH values (*i.e.* between pH = 2 and pH = 9), and become negative under alkaline pH conditions (Figure 4). This variation for alkaline pH values is generated by the deprotonation of the edge-sites of LAP.[40] LAP-CB-0.5CEC and LAP-CB-4CEC exhibit three ranges of ZP values. ZP values are positive for acidic pH values, close to 0 between pH ≈ 3.5 and pH ≈ 7.5, and are negative for alkaline pH values (Figure 4).

The speciation of CB (Fig S1) is in accordance with these variations. Therefore, the variation of the surface charge of LAP-CBs is solely generated by the speciation of CB for the pH values < 10, and the deprotonotation of edge-sites is only significant for strong alkaline pH values.[41,42] It should be mentioned that the variation of ZP values are more important for LAP-CB-4CEC in comparison with LAP-CB-0.5CEC due to the higher amount of CB adsorbed onto the surface for the highest CB load (Figure 3).

Adsorption experiments

Impact of pH. The impact of pH on the single-solute adsorption of Cs^+, Co^{2+} and Sr^{2+} onto LAP and LAP-CB-4CEC is presented Figure 5. The adsorbed amount of Sr^{2+} onto LAP is important and increases from 58 to 98 % at pH = 2.3 and pH = 12.2 respectively. The same pattern is observed onto LAP-CB-4CEC with an increase of the adsorbed percentage from 19 to 95 % at pH = 2.4 and pH = 11.8 respectively. In the same way, the adsorption of Cs^+ onto LAP-CB-4CEC strongly increases under alkaline pH conditions, from 5 to 35% at pH=2.3 and pH=11.9, respectively. Conversely, the adsorption of Cs^+ onto LAP is very limited (*i.e.* between 5.5 and 9.9 %) and the increase of adsorption percentage under alkaline conditions is not significant.

The adsorption of Co^{2+} onto LAP is very poor and due to the precipitation of Co^{2+} when pH > 7.5,[11] it can be considered that the pH value has a weak impact on the adsorption extent of Co^{2+} onto LAP.

In the same way the adsorption of Co^{2+} onto LAP-CB-4CEC is not pH-dependent with high adsorption percentage (*i.e.* between 80 and 99 %) whatever the pH value, except for the most acidic solution, for which the adsorption of Co^{2+} is very low (*i.e.* < 2%). As previously observed with the variation of ZP values of LAP and two LAP-CBs, pH values play a key role on the speciation of the surfactant and in a less important manner on the deprotonation of edge-sites of LAP (Figure 4). The modification of the surfactant charge state is particularly important for pH > 3.2, due its zwitterionic form since this pH value. Cations such as Sr^{2+} and Cs^+ are obviously sensible to this modification of speciation. However, it is not the case for Co^{2+}, indicating that the adsorption of Co^{2+} onto adsorbents is less sensible to the amount of available negative charges even if Co^{2+} is obviously cationic.[11]

Single-solute interactions. The single-solute adsorption of each selected contaminant has been investigated onto LAP and LAP-CBs.

The adsorption isotherms of Cs^+ are presented Figure 6. Regardless the adsorbent, the adsorption of Cs^+ is not favorable with significant equilibrium concentrations even for the lower initial concentrations tested. However, the adsorption capacity significantly varies between each adsorbent. The lowest adsorption capacity is observed for LAP (*i.e.* 0.055 mmol.g^{-1}), whereas the adsorption capacities onto LAP-CBs are much higher.

The increase of the surfactant load significantly decreases the adsorption capacity with maximal adsorbed concentration of 0.20 and 0.14 mmol g^{-1} at 0.5 and 4 CEC respectively. The best fit of experimental data is performed with Freundlich equation (Table 1). The increase of K_F values between LAP and LAP-CB-0.5CEC from 0.08 to 0.32 (mg.g^{-1})/(mg.L^{-1})^n points out the better affinity of Cs^+ to LAP-CBs than LAP.

The same trend can be observed for the single-solute adsorption of Co^{2+} (Figure 7). Thus, the lowest adsorption capacity with unfavorable adsorption behavior is displayed onto LAP with a maximal adsorption capacity of 0.09 mmol g^{-1} (Figure 7). Conversely, onto LAP-CBs, the adsorption is more favorable with low equilibrium concentrations before reaching a saturation plateau at different levels for each CB load. At 0.5 and 1 CEC of CB, the adsorption capacity is equal to 0.37 and 0.34 mmol g^{-1} respectively, and at 2 and 4 CEC, the adsorption capacity is equal to 0.24 and 0.27 mmol g^{-1}. Hence, the modification of the surfactant arrangement (Figure 1) impacts the adsorption capacity of Co^{2+}. This variation between LAP and LAP-CBs is also expressed in the model fits. The adsorption onto LAP is well-fitted by the Freundlich model whereas the adsorption onto LAP-CBs is properly fitted by the Langmuir equation (Table 1). It should be mentioned that the mean free energy (E) is below 8 kJ.mol^{-1} only for the adsorption of Co^{2+} onto LAP. Therefore, the organo-modification of LAP strongly modifies the affinity between Co^{2+} and the sorbent.

The adsorption of Sr^{2+} onto the different adsorbents show two distinct regimes with one displaying a gradual growth of adsorbed Sr^{2+} with equilibrium Sr^{2+} concentrations, whereas the second one points out a steady state for the highest initial concentrations (Figure 8). However, the saturation of each adsorbent occurs at different adsorbed amounts. The highest adsorption capacity of Sr^{2+} is displayed onto LAP with a value equal to 0.26 mmol g^{-1} (i.e. corresponding to 70% of the CEC of LAP); whereas onto LAP-CBs, the adsorption capacity decreases with increasing the surfactant load from 0.23 to 0.16 mmol.g^{-1} at 0.5 and 4 CEC of CB respectively. The adsorption of Sr^{2+} is well-fitted by the Langmuir equation exhibiting chemisorption

(E > 8kJ mol^{-1}) and spontaneous adsorption (ΔG° < 0) regardless the sorbent (Table 1).

Competitive adsorption. The competitive adsorption was carried out with ternary solutions. The competitive adsorption isotherms of Co^{2+}, Sr^{2+} and Cs^{+} are presented Figures S4-6. In order to assess the impact of competition on the adsorption of each contaminant, Figure 9 summarizes the adsorption isotherms of each contaminant in both single-solute and ternary solutions onto LAP and LAP-CB-0.5CEC. A competitive effect is observed in the same extent whatever the surfactant load onto LAP-CB (Figures S4-6, Table 1).

The adsorption of Co^{2+} on both LAP and LAP-CBs is not impacted by the competition with Cs^{+} and Sr^{2+} in the used concentration range. Indeed, both the adsorption capacity and the adsorption behavior are identical for mono-molecular and ternary solutions whatever the adsorbent (Figure 9). It could indicate different adsorption sites of Co^{2+}, or a strong selectivity of the adsorbent.[43] Conversely, the adsorption of Cs^{+} onto LAP-CBs is affected by the competition. An important drop in the adsorption capacity is observed, from 0.2 to 0.1 mmol g^{-1} in single-solute and ternary solutions respectively (Figure 9). The affinity between Cs^{+} and the adsorbent remains close but a competitive effect can be assumed. In the same way, the adsorption of Sr^{2+} onto LAP-CBs is impacted by the competition. The adsorption capacity decreases from 0.25 to 0.12 mmol g^{-1} in single-solute and ternary solution experiments respectively.

Table 1: Single-solute (Mono) and competitive (Comp) sorption model parameters for sorption of Co^{2+}, Cs^{+} and Sr^{2+} onto LAP and LAP-CBs

			Langmuir				Freundlich			Dubinin-Raduskevich		
			Q_{max}	K_L	ΔG°	r²	n	K_F	r²	Q_m	E	r²
			mmol g^{-1}	L mmol^{-1}	kJ mol^{-1}			(mg.g^{-1})/(mg.L^{-1})^n		mmol.g^{-1}	kJ.mol^{-1}	
Co^{2+}	Mono	LAP	0.141	4.2	-3.52	0.827	1.33	0.21	0.997	0.069	6.546	0.946
		0.5CEC	0.397	244.4	-13.40	0.996	1.51	5.89	0.905	0.796	8.715	0.970
		1CEC	0.377	196.5	-12.87	0.989	1.44	6.30	0.932	0.948	8.143	0.930
		2CEC	0.294	192.4	-12.82	0.998	1.65	2.60	0.775	0.703	8.107	0.923
		4CEC	0.263	447.7	-14.88	0.986	3.30	0.71	0.850	0.362	10.660	0.964
	Comp	LAP	0.158	3.7	-3.16	0.843	1.21	0.26	0.979	0.084	5.013	0.979
		0.5CEC	0.394	151.9	-12.24	0.977	1.37	6.96	0.813	1.184	6.681	0.935
		1CEC	0.352	193.1	-12.83	0.993	1.55	4.09	0.768	1.010	6.901	0.916
		2CEC	0.290	259.3	-13.55	0.999	1.96	1.64	0.882	0.388	8.771	0.939
		4CEC	0.233	251.9	-13.48	0.996	2.52	0.75	0.865	0.102	9.449	0.970
Cs^{+}	Mono	LAP	0.077	4.9	-3.90	0.949	1.86	0.08	0.984	0.056	3.769	0.938
		0.5CEC	0.209	23.8	-7.73	0.961	2.38	0.32	0.986	0.302	8.704	0.945
		1CEC	0.192	17.9	-7.03	0.970	2.10	0.30	0.986	0.133	7.857	0.929
		2CEC	0.179	15.7	-6.71	0.965	2.04	0.28	0.994	0.125	7.454	0.944
		4CEC	0.147	19.8	-7.28	0.949	2.69	0.19	0.993	0.099	9.285	0.932
	Comp	LAP	0.052	14.3	-6.49	0.989	2.02	0.08	0.981	0.047	6.131	0.994
		0.5CEC	0.111	11.7	-5.99	0.972	2.60	0.13	0.994	0.088	6.565	0.935
		1CEC	0.097	15.1	-6.62	0.986	2.81	0.12	0.987	0.085	6.622	0.971
		2CEC	0.087	12.0	-6.06	0.944	3.39	0.09	0.956	0.066	7.495	0.867
		4CEC	0.019	17.3	-7.17	0.996	2.61	0.02	0.643	0.025	6.742	0.859
Sr^{2+}	Mono	LAP	0.264	351.1	-14.29	0.998	1.95	1.59	0.463	0.420	11.471	0.997
		0.5CEC	0.229	383.1	-14.50	0.996	2.64	0.77	0.856	0.282	10.314	0.929
		1CEC	0.202	154.9	-12.29	0.990	2.51	0.56	0.905	0.201	9.901	0.932
		2CEC	0.188	124.7	-11.76	0.988	2.44	0.51	0.917	0.192	9.449	0.955
		4CEC	0.163	100.5	-11.23	0.986	2.88	0.34	0.786	0.166	9.285	0.917
	Comp	LAP	0.284	181.6	-12.68	0.984	1.79	2.03	0.622	0.792	7.036	0.772
		0.5CEC	0.121	564.1	-15.44	0.999	3.04	0.32	0.576	0.189	9.366	0.684
		1CEC	0.122	154.1	-12.28	0.999	2.11	0.42	0.819	0.186	7.538	0.934
		2CEC	0.101	113.6	-11.54	0.999	1.97	0.36	0.783	0.165	6.901	0.929
		4CEC	0.070	194.4	-12.84	0.999	2.48	0.19	0.745	0.102	7.762	0.872

However, this trend is not visible for the adsorption of Sr^{2+} onto LAP. On LAP-CBs, it exists a competitive effect between Cs^{+} and Sr^{2+}, and the adsorption capacities reach a saturation around 0.25 mmol g^{-1} for Sr^{2+} or Cs^{+} alone, or in competition. It is interesting to note that despite their different valence, the adsorption capacity remains the same. Therefore, it seems that the limiting factor is more the availability of adsorption sites rather than global charge.

The sorption mechanisms remains identical whatever the composition of the solution, even if the adsorption capacities is modified (Table 1), as expressed by the proper fit with the same model for both single-solute and competitive adsorption tests.

Desorption experiments

Desorption experiments have been performed with adsorbent samples that were previously in interaction with the highest starting concentration of Co^{2+}, Cs^{+} and Sr^{2+} in single-solute experiments.

After drying, sorbent samples were put in three different types of solutions in order to evaluate the impact of inorganic salts and their valence on desorption behavior. The results are presented in Figure 10.

The desorption behavior of each contaminant varies both with the adsorbent (*i.e.* LAP or LAP-CBs) and the initial composition of the solution.

For example, desorption of Co^{2+} is important for the LAP samples, with desorbed percentages between 15 and 42%, although its desorption from LAP-CBs is below 1.5 % whatever the surfactant load or the initial composition of the solution. A slight (but non-significant) increase tendency of the desorbed amount is observed with increasing the CB load (Figure 10).

The desorption behavior of Sr^{2+} is less impacted by the CB load than the composition of the solution. For a same adsorbent, the highest desorbed amount is systematically observed in $CaCl_2$ solution, and the lowest in pure water. The desorption in NaCl solution is intermediate. This indicates that the valence of the inorganic cation plays a key role in the desorption of Sr^{2+}.

This trend can also be described on the desorption behavior of Cs^+. Systematically, the desorption percentage is the highest in NaCl solution, but the desorption percentage is also very high in pure water and $CaCl_2$ solution. The Cs^+ cation is therefore highly desorbed whatever the release solution tested, even higher values are noticed for inorganic salt with the same valence (Figure 10).

Sorption mechanisms

Based on the adsorption and desorption results, the sorption mechanisms of each contaminants can be discussed. The adsorption of Sr^{2+} onto LAP is favorable, properly fitted by the Langmuir model and the adsorption capacity corresponds to 70% of the CEC of LAP (Figure 8). Moreover, the desorption results exhibit that even if the desorbed amount of Sr^{2+} is very weak in pure water or NaCl solution, the presence of Ca^{2+} strongly increases the desorption of Sr^{2+} (Figure 10). As a consequence, desorption increases with the presence of an inorganic cation with the same valence than the adsorbed contaminant. All these results demonstrate that Sr^{2+} is adsorbed through cation exchange onto LAP. The same results were observed onto LAP-CBs (Figure 8). However, we don't have the information about the CEC of these adsorbents, and their adsorption capacities of Sr^{2+} were lower than that of LAP. It indicates the impact of the arrangement of the surfactant within the LAP layer, which could hinder the cation exchange mechanism. However, Sr^{2+} is also adsorbed through cation exchange onto LAP-CBs, and may be used as a probe of the CEC of each adsorbent, due to its selective adsorption instead of Na+, the compensation ion of LAP.[44] The adsorption of Co^{2+} onto LAP is not favorable and seems to be dependent on the solid/water partition. As a result, none competitive effect has been observed as well as high desorption percentages whatever the composition of the solution (Figure 10). Co^{2+} is therefore adsorbed through weak electrostatic bindings onto LAP. The organo-modification of LAP strongly modifies the affinity of the materials with Co^{2+}. Co^{2+} is indeed efficiently adsorbed onto LAP-CBs in a wide range of concentration with very low equilibrium concentrations. The desorption percentages of Co^{2+} are also very low whatever the composition of the solution or the CB load. However, a decrease of the adsorption capacity is noticed for higher CB loads (Figures 7 and S6). As previously explained for the adsorption of Sr^{2+}, high surfactant load could diminish the availability of adsorption sites. Yet, the addition of CB within the layers dramatically changes the affinity of the material with Co^{2+}. We can therefore assume that Co^{2+} is adsorbed through chelation mechanism with a specific chemical function of the surfactant.[45,46] Finally, the adsorption of Cs^+ onto the selected adsorbents is more difficult to understand. The adsorption of Cs^+ onto LAP is poorly performed (Figures 6 and S4) as already demonstrated on pure clay minerals.[47] Cs^+ is generally adsorbed onto surface defaults of clay minerals.[48] However, LAP is a synthetic material which presents only few structural defaults. The high desorption of Cs^+ from LAP whatever the releasing solution indicates that the adsorption is probably performed through physisorption (Figure 10). Then, the desorption percentage is systematically the highest in NaCl saline solutions, especially for LAP-CBs. Moreover, the competition with Sr^{2+} is very important onto these adsorbents. The adsorption of Cs^+ is therefore partially performed through cation exchange, especially onto LAP-CBs, as revealed by the decreasing adsorption capacity with increasing the CB load (i.e. as displayed by Sr^{2+} adsorption capacity). But a significant fraction of Cs^+ is also adsorbed through weak electrostatic interaction,[49] as exhibited by the adsorption isotherms of Cs^+, which are moderately favorable.

Conclusions

In this work, the interest of the organo-modification of a synthetic clay mineral was demonstrated in order to develop green, safe and multi-skilled adsorbents for the removal of radionuclides. Indeed, LAP-CBs exhibit favorable adsorption properties for Co^{2+}, Sr^{2+} and Cs^+ in comparison with the raw LAP which only allows a significant adsorption of Sr^{2+}. Moreover, this adsorption seems to be specific and highly stable especially for Co^{2+}, given the strong binding with CB.

However, our results demonstrate that the CB load, which impacts the CB arrangement within the layers of LAP, is of high concern for the availability of adsorption sites in one hand, and for the conservation of the cation exchange properties on the other hand. It appears that the lowest surfactant load presents the highest adsorption capacities of Co^{2+} and Cs^+. This minimal CB load seems to avoid the recombination of surfactant molecules and also the steric hindrance in the interlayer space. The monolayer arrangement also ensures a good further stability of the hybrid materials. Oppositely, the important amount of surfactant adsorbed onto the surface for higher CB load raises hard questions about the long-term stability of the organo-clays, especially in saline solutions.

In the tested ternary solutions, a competitive effect between Cs^+ and Sr^{2+} was observed for the adsorption onto LAP-CBs. As these two contaminants were adsorbed through cation exchange, this competitive impact should be taken into consideration for the evaluation of the suitability of the developed adsorbent for the treatment of complex solutions. Thus, the selectivity of Sr^{2+} and Cs^+ adsorption in comparison with other inorganic cations would be of high concern.

The proposed LAP-CB, especially LAP-CB-0.5CEC, could therefore represent a cheap, green and easy to prepare adsorbent for the removal of radionuclides from LLRW.

However, further tests remain necessary, especially on the adsorption capacities in complex solutions (*i.e.* real effluents) and on the aging of the adsorbent during the storage, especially when exposed to radioactivity. Indeed, the use of this green adsorbent for the further storage of radionuclides may significantly reduce the environmental footprint of nuclear waste packages.

Conflicts of interest

There are no conflicts to declare.

Acknowledgements

The ONET Technologies company is gratefully thanked for funding this work.

References

1 E. L. Gershey, R. C. Klein, E. Party and A. Wilkerson, *Low-level radioactive waste*, Van Nostrand Reinhold Co., New York, NY, 1990.
2 R. C. Ewing, R. A. Whittleston and B. W. D. Yardley, *Elements*, 2016, **12**, 233–237.
3 S. Singh, S. Eapen, V. Thorat, C. P. Kaushik, K. Raj and S. F. D'Souza, *Ecotoxicology and Environmental Safety*, 2008, **69**, 306–311.
4 S. Righi, P. Lucialli and L. Bruzzi, *Journal of Environmental Radioactivity*, 2005, **82**, 167–182.
5 I. Ali, M. Asim and T. A. Khan, *Journal of Environmental Management*, 2012, **113**, 170–183.
6 R. O. A. Rahman, H. A. Ibrahium and Y.-T. Hung, *Water*, 2011, **3**, 551–565.
7 X.-H. Fang, F. Fang, C.-H. Lu and L. Zheng, *Nuclear Engineering and Technology*, 2017, **49**, 556–561.
8 H. Faghihian, M. Moayed, A. Firooz and M. Iravani, *Journal of Colloid and Interface Science*, 2013, **393**, 445–451.
9 L. Zhang, J. Wei, X. Zhao, F. Li, F. Jiang, M. Zhang and X. Cheng, *Chemical Engineering Journal*, 2016, **302**, 733–743.
10 T. T. H. Dang, C.-W. Li and K.-H. Choo, *Separation and Purification Technology*, 2016, **157**, 209–214.
11 B. Ma, S. Oh, W. S. Shin and S.-J. Choi, *Desalination*, 2011, **276**, 336–346.
12 H. Long, P. Wu and N. Zhu, *Chemical Engineering Journal*, 2013, **225**, 237–244.
13 A.-A. M. Abdel-Karim, A. A. Zaki, W. Elwan, M. R. El-Naggar and M. M. Gouda, *Applied Clay Science*, 2016, **132**, 391–401.
14 T. Thiebault, R. Guégan and M. Boussafir, *Journal of Colloid and Interface Science*, 2015, **453**, 1–8.
15 M. Claverie, J. Garcia, T. Prevost, J. Brendlé and L. Limousy, *Materials*, 2019, **12**, 1399.
16 T. Thiebault, M. Boussafir, R. Guégan, C. Le Milbeau and L. Le Forestier, *Environ. Sci.: Water Res. Technol.*, 2016, **2**, 529–538.
17 W. M. Ye, Z. J. Zheng, B. Chen, Y. G. Chen, Y. J. Cui and J. Wang, *Applied Clay Science*, 2014, **101**, 192–198.
18 S. Gin, A. Abdelouas, L. J. Criscenti, W. L. Ebert, K. Ferrand, T. Geisler, M. T. Harrison, Y. Inagaki, S. Mitsui, K. T. Mueller, J. C. Marra, C. G. Pantano, E. M. Pierce, J. V. Ryan, J. M. Schofield, C. I. Steefel and J. D. Vienna, *Materials Today*, 2013, **16**, 243–248.
19 P. Sellin and O. X. Leupin, *Clays and Clay Minerals*, 2013, **61**, 477–498.
20 J. Bruno, D. Arcos and L. Duro, *Processes and features affecting the near field hydrochemistry. Groundwater-bentonite interaction*, Swedish Nuclear Fuel and Waste Management Co., 1999.
21 P. Wersin, E. Curti and C. A. J. Appelo, *Applied Clay Science*, 2004, **26**, 249–257.
22 S. Staunton, C. Dumat and A. Zsolnay, *Journal of Environmental Radioactivity*, 2002, **58**, 163–173.
23 T. de Oliveira, R. Guégan, T. Thiebault, C. L. Milbeau, F. Muller, V. Teixeira, M. Giovanela and M. Boussafir, *Journal of Hazardous Materials*, 2017, **323**, **Part A**, 558–566.
24 R. Guégan, M. Giovanela, F. Warmont and M. Motelica-Heino, *Journal of Colloid and Interface Science*, 2015, **437**, 71–79.
25 L. B. de Paiva, A. R. Morales and F. R. Valenzuela Díaz, *Applied Clay Science*, 2008, **42**, 8–24.
26 S. M. Lee and D. Tiwari, *Applied Clay Science*, 2012, **59–60**, 84–102.
27 M. Jaber, J. Miehé-Brendlé, L. Michelin and L. Delmotte, *Chem. Mater.*, 2005, **17**, 5275–5281.
28 L. Ma, Q. Chen, J. Zhu, Y. Xi, H. He, R. Zhu, Q. Tao and G. A. Ayoko, *Chemical Engineering Journal*, 2016, **283**, 880–888.
29 A. R. McLauchlin and N. L. Thomas, *Polymer Degradation and Stability*, 2009, **94**, 868–872.
30 M. J. Sanchez-Martin, M. S. Rodriguez-Cruz, M. S. Andrades and M. Sanchez-Camazano, *Applied Clay Science*, 2006, **31**, 216–228.
31 B. K. G. Theng, *Clays and Clay Minerals*, 1982, 1–10.
32 H. I. Leidreiter, B. Gruning and D. Kaseborn, *International Journal of Cosmetic Science*, 1997, **19**, 239–253.
33 S. Xia, Y. Zhou, E. Eustance and Z. Zhang, *Scientific Reports*, 2017, **7**, 13491.
34 T. Thiebault, M. Boussafir, L. Le Forestier, C. Le Milbeau, L. Monnin and R. Guégan, *RSC Adv.*, 2016, **6**, 65257–65265.
35 A. Sdiri, T. Higashi, T. Hatta, F. Jamoussi and N. Tase, *Chemical Engineering Journal*, 2011, **172**, 37–46.
36 A. R. McLauchlin and N. L. Thomas, *Journal of Colloid and Interface Science*, 2008, **321**, 39–43.
37 G. Lagaly, *Solid State Ionics*, 1986, **22**, 43–51.
38 W. Xie, Z. Gao, K. Liu, W.-P. Pan, R. Vaia, D. Hunter and A. Singh, *Thermochimica Acta*, 2001, **367–368**, 339–350.
39 J. Zhu, P. Zhang, Y. Qing, K. Wen, X. Su, L. Ma, J. Wei, H. Liu, H. He and Y. Xi, *Applied Clay Science*, 2017, **141**, 265–271.
40 S. L. Tawari, D. L. Koch and C. Cohen, *Journal of Colloid and Interface Science*, 2001, **240**, 54–66.
41 P. Mongondry, T. Nicolai and J.-F. Tassin, *Journal of Colloid and Interface Science*, 2004, **275**, 191–196.
42 S. Jatav and Y. M. Joshi, *Applied Clay Science*, 2014, **97–98**, 72–77.
43 V. C. Srivastava, I. D. Mall and I. M. Mishra, *Colloids and Surfaces A: Physicochemical and Engineering Aspects*, 2008, **312**, 172–184.
44 W. Luo, A. Inoue, T. Hirajima and K. Sasaki, *Applied Surface Science*, 2017, **394**, 431–439.
45 G. L. Woodward, C. L. Peacock, A. Otero-Fariña, O. R. Thompson, A. P. Brown and I. T. Burke, *Geochimica et Cosmochimica Acta*, 2018, **238**, 270–291.
46 M. K. Uddin, *Chemical Engineering Journal*, 2017, **308**, 438–462.
47 H. Mukai, A. Hirose, S. Motai, R. Kikuchi, K. Tanoi, T. M.

View Article Online
DOI: 10.1039/C9GC02243K

Nakanishi, T. Yaita and T. Kogure, *Scientific Reports*, 2016, **6**, srep21543.
48 H. Mukai, S. Motai, T. Yaita and T. Kogure, *Applied Clay Science*, 2016, **121**, 188–193.
49 Q. H. Fan, M. Tanaka, K. Tanaka, A. Sakaguchi and Y. Takahashi, *Geochimica et Cosmochimica Acta*, 2014, **135**, 49–65.

View Article Online
DOI: 10.1039/C9GC02243K

ARTICLE

Figure captions

Figure 1: X-ray diffraction patterns of LAP and LAP-CBs for different surfactant loads (from 0.5 to 4 CEC)

Figure 2: DTG curves for LAP and LAP-CBs between 0 and 900°C with a heating rate of 2°C.min^{-1}

Figure 3: Evolution of the organic content in wt% with the increase of initial surfactant load during synthesis. Numbers into brackets correspond to the total adsorbed surfactant compared with the CEC of LAP.

Figure 4: ZP values as a function of the pH for LAP, LAP-CB-0.5CEC and LAP-CB-4CEC, the arrows at the bottom of the figure marks the speciation of CB

Figure 5: Single-solute adsorption of Cs^+, Co^{2+} and Sr^{2+} onto LAP (red circles) and LAP-CB-4CEC (blue squares) as a function of pH, the adsorbed amount (in %) represents the removal rate from aqueous phase, the arrows at the bottom of the figure mark the speciation of CB

Figure 6: Single-solute adsorption isotherms of Cs^+ onto LAP and LAP-CBs, dashed dark lines represent the Langmuir fits

Figure 7: Single-solute adsorption isotherms of Co^{2+} onto LAP and LAP-CBs, dashed dark lines represent the Langmuir fits

Figure 8: Single-solute adsorption isotherms of Sr^{2+} onto LAP and LAP-CBs, dashed dark lines represent the Langmuir fits

Figure 9: Adsorption isotherms of Co^{2+} (triangles), Cs^+ (squares) and Sr^{2+} (circles) in single-solute (open symbols) and competitive (closed symbols) solutions on LAP (A) and LAP-CB-0.5CEC (B). Dashed dark lines represent the Langmuir fits.

Figure 10: Desorption percentage of Co^{2+} (dark rods), Sr^{2+} (gray rods) and Cs^+ (light gray rods) as a function of the adsorbent and the release solutions.

View Article Online
DOI: 10.1039/C9GC02243K

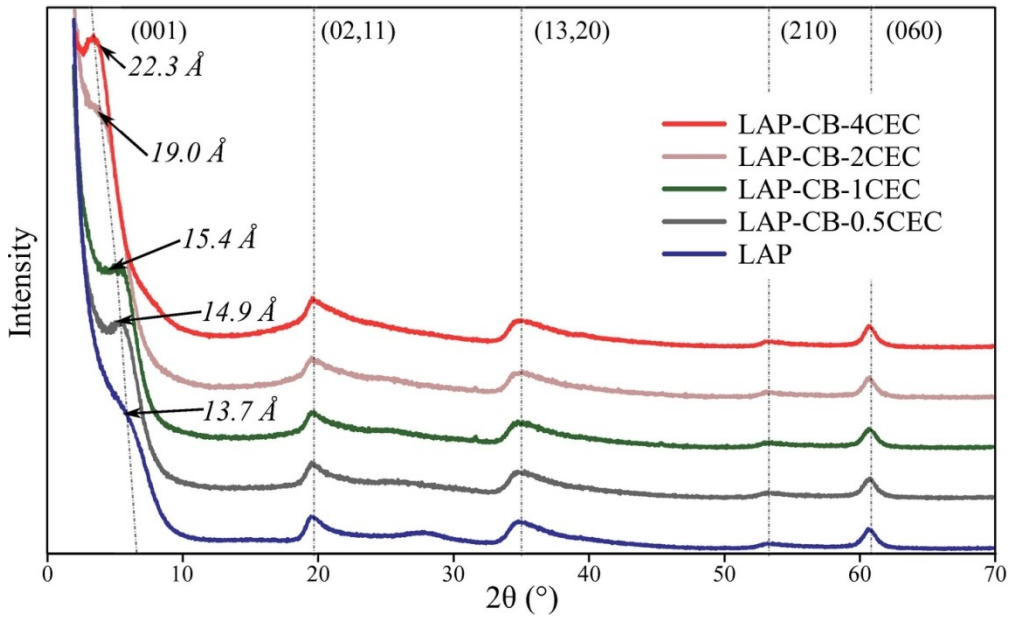

Figure 1: X-ray diffraction patterns of LAP and LAP-CBs for different surfactant loads (from 0.5 to 4 CEC)

122x74mm (300 x 300 DPI)

View Article Online
DOI: 10.1039/C9GC02243K

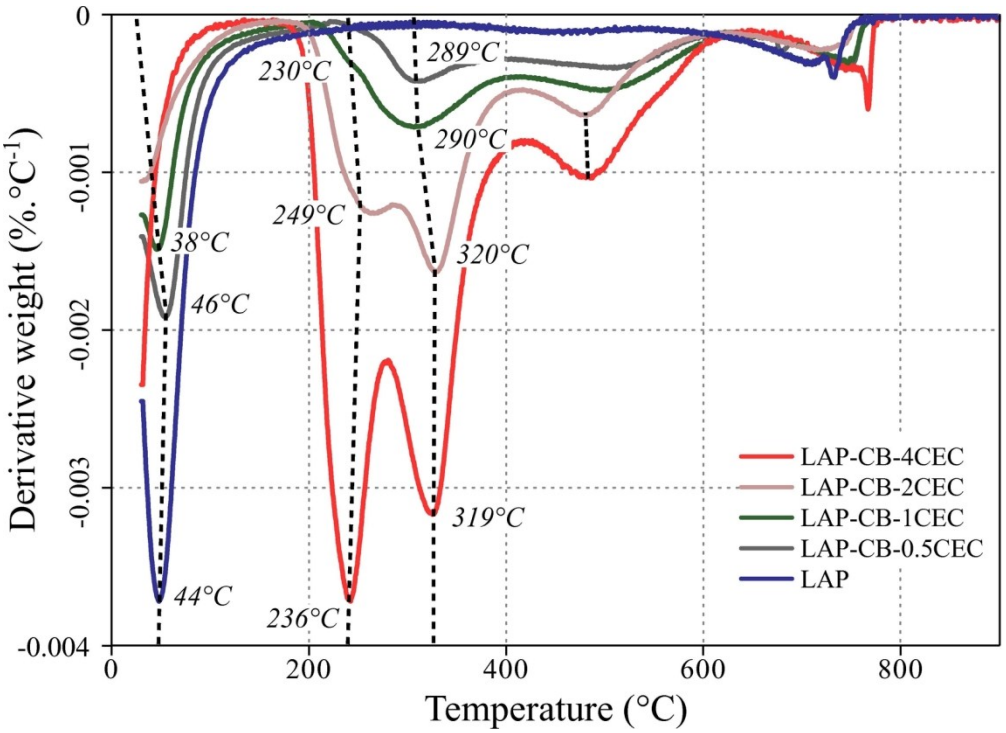

Figure 2: DTG curves for LAP and LAP-CBs between 0 and 900°C with a heating rate of 2°C.min-1

150x108mm (300 x 300 DPI)

View Article Online
DOI: 10.1039/C9GC02243K

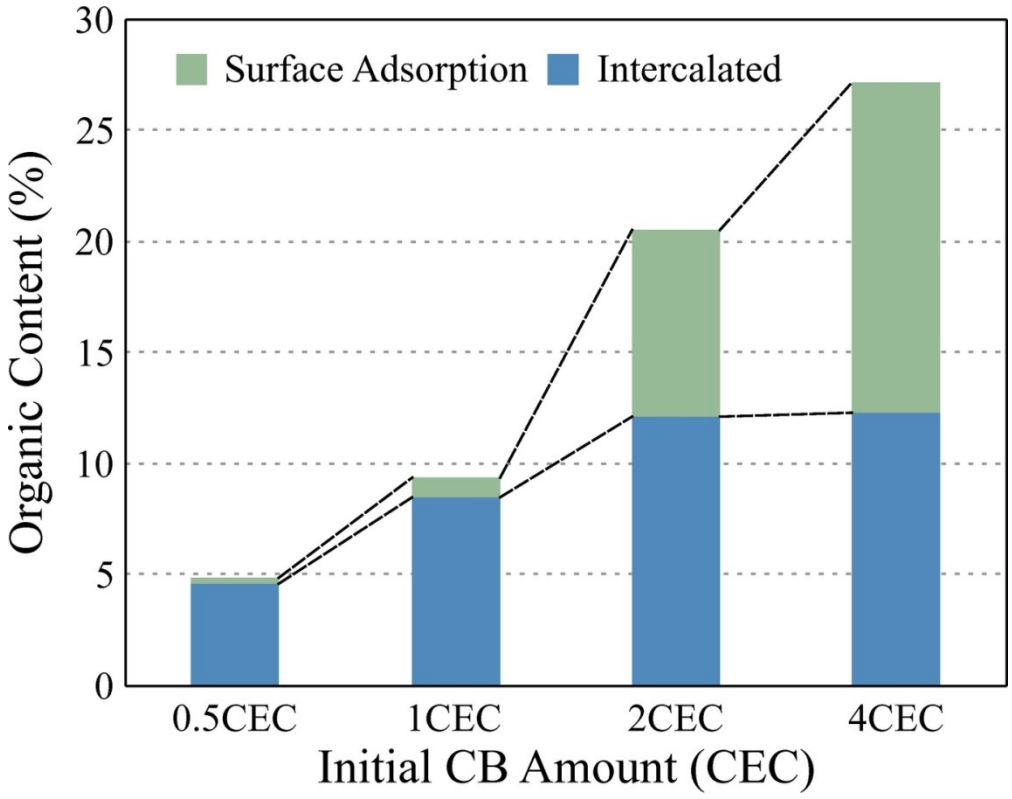

Figure 3: Evolution of the organic content in wt% with the increase of initial surfactant load during synthesis. Numbers into brackets correspond to the total adsorbed surfactant compared with the CEC of LAP.

116x91mm (300 x 300 DPI)

View Article Online
DOI: 10.1039/C9GC02243K

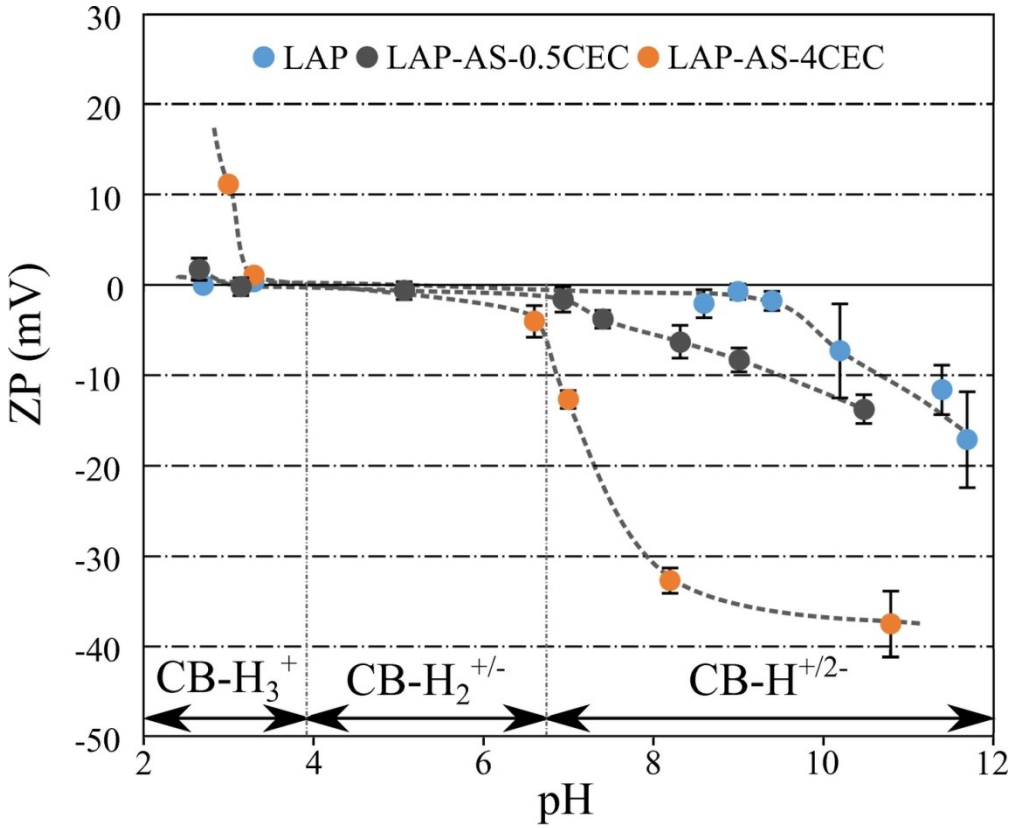

Figure 4: ZP values as a function of the pH for LAP, LAP-CB-0.5CEC and LAP-CB-4CEC, the arrows at the bottom of the figure marks the speciation of CB

122x100mm (300 x 300 DPI)

View Article Online
DOI: 10.1039/C9GC02243K

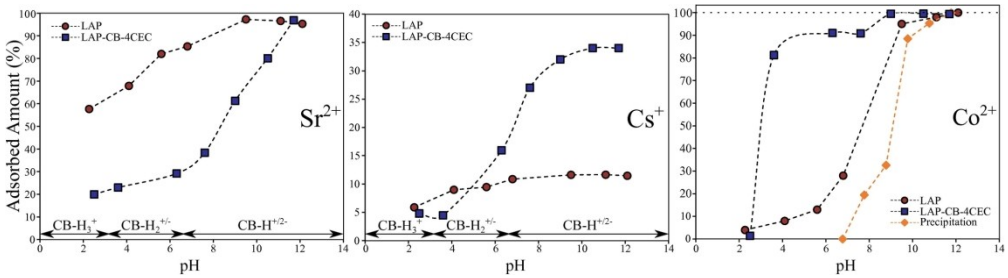

Figure 5: Single-solute adsorption of Cs+, Co2+ and Sr2+ onto LAP (red circles) and LAP-CB-4CEC (blue squares) as a function of pH, the adsorbed amount (in %) represents the removal rate from aqueous phase, the arrows at the bottom of the figure mark the speciation of CB

189x51mm (300 x 300 DPI)

View Article Online
DOI: 10.1039/C9GC02243K

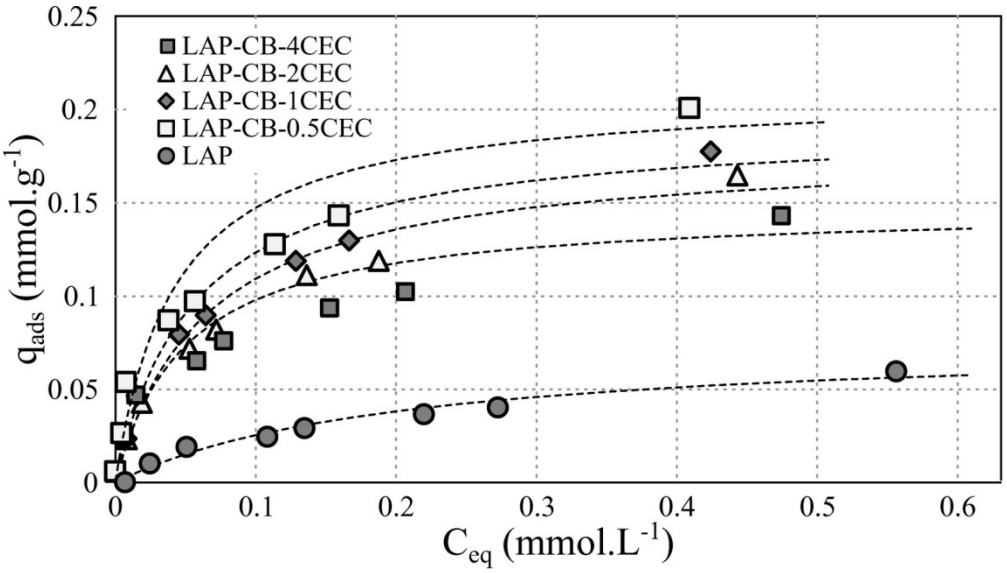

Figure 6: Single-solute adsorption isotherms of Cs+ onto LAP and LAP-CBs, dashed dark lines represent the Langmuir fits

144x81mm (300 x 300 DPI)

View Article Online
DOI: 10.1039/C9GC02243K

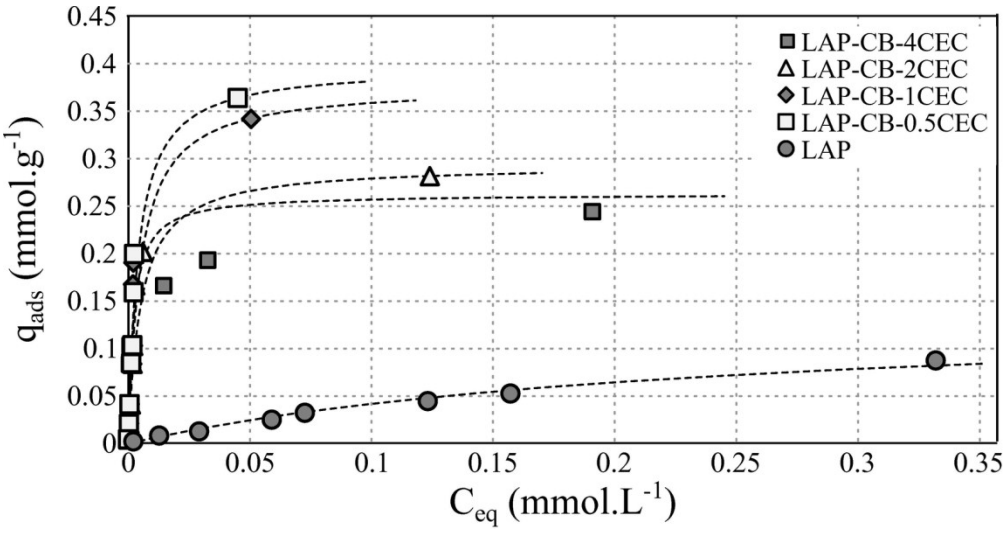

Figure 7: Single-solute adsorption isotherms of Co2+ onto LAP and LAP-CBs, dashed dark lines represent the Langmuir fits

147x76mm (300 x 300 DPI)

View Article Online
DOI: 10.1039/C9GC02243K

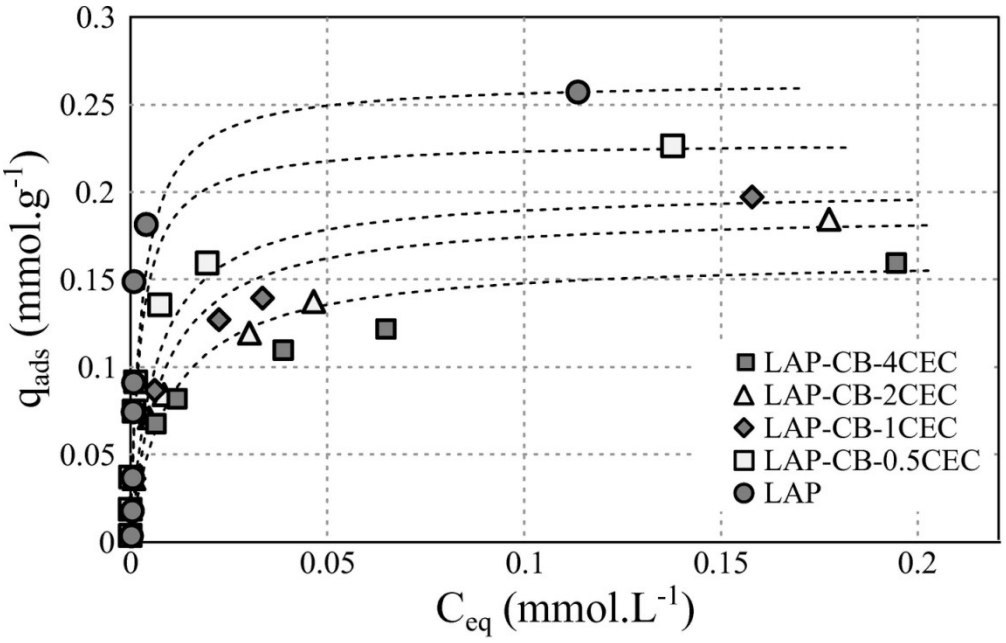

Figure 8: Single-solute adsorption isotherms of Sr2+ onto LAP and LAP-CBs, dashed dark lines represent the Langmuir fits

120x76mm (300 x 300 DPI)

View Article Online
DOI: 10.1039/C9GC02243K

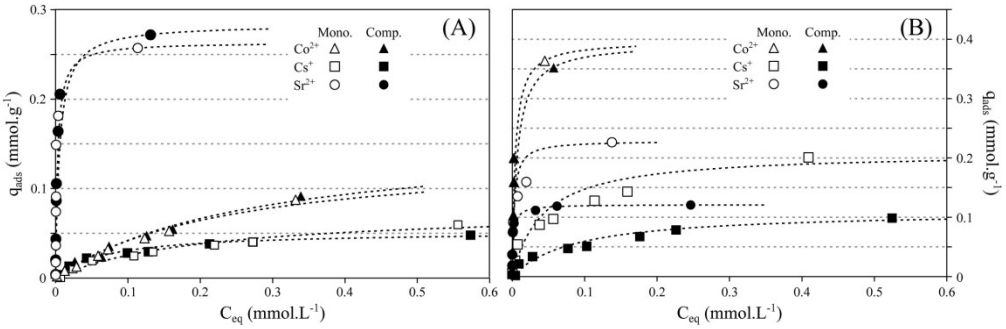

Figure 9: Adsorption isotherms of Co2+ (triangles), Cs+ (squares) and Sr2+ (circles) in single-solute (open symbols) and competitive (closed symbols) solutions on LAP (A) and LAP-CB-0.5CEC (B). Dashed dark lines represent the Langmuir fits.

203x65mm (300 x 300 DPI)

View Article Online
DOI: 10.1039/C9GC02243K

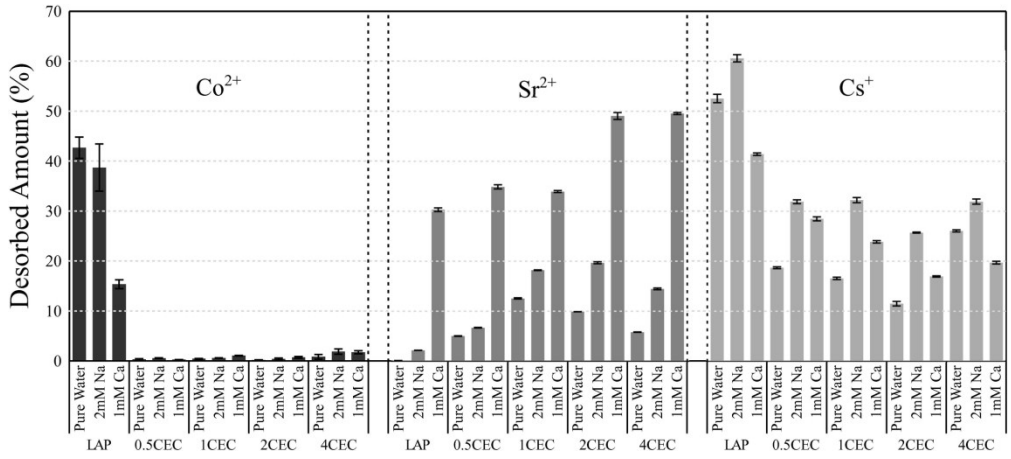

Figure 10: Desorption percentage of Co2+ (dark rods), Sr2+ (gray rods) and Cs+ (light gray rods) as a function of the adsorbent and the release solutions.

191x85mm (300 x 300 DPI)